Asian Journal of Research and Reviews in Physics

4(4): 19-31, 2021; Article no.AJR2P.71413
ISSN: 2582-5992

Thin Films Growth of $SnO_2:F/CdS/CdTe$, and Studies of Their Physical and Optical Properties using Spray Pyrolysis Techniques

A. O. Musa[1], A. B. Ahmed[2], Mansur Said[3*], Mani Tsoho[4] and A. B. Suleiman[5]

[1]Physics Department, Bayero University Kano, Nigeria.
[2]Physics Department, Gombe State University Kano, Nigeria.
[3]Physics Department, Yusuf Maitama Sule University Kano, Nigeria.
[4]Physics Department Saadatu Rimi College of Education Kano, Nigeria.
[5]Physics Department, Federal University Dutse, Nigeria.

Authors' contributions

This work was carried out in collaboration among all authors. All authors read and approved the final manuscript.

Article Information

DOI: 10.9734/AJR2P/2021/v4i430149
Editor(s):
(1) Dr. Jelena Purenovic, Kragujevac University, Serbia.
(2) Dr. Khalil Kassmi, Mohamed Premier University, Morocco.
(3) Prof. Shi-Hai Dong, National Polytechnic Institute, Mexico.
Reviewers:
(1) Dimitra Vernardou, Hellenic Mediterranean University, Greece.
(2) Mahdi Hasan Suhail, University of Baghdad, Egypt.
Complete Peer review History: https://www.sdiarticle4.com/review-history/71413

Original Research Article

Received 03 June 2021
Accepted 06 August 2021
Published 12 August 2021

ABSTRACT

Fluorine doped tin oxide,$SnO_2:F$ (FTO),Cadmium Sulphide (CdS) and Cadmium Telluride CdTe thin films have been deposted on Soda Lime glass substrate at $500℃, 400℃$ and $300℃$ respectively by spray pyrolysis (SP) technique and are important semiconductor materials in optoelectronic devices such as optical sensors, light-emitting diodes, transistors and photovoltaic cells. FTO, CdS and CdTe thin films were characterized by various techniques such as X-ray diffraction, SEM and optical studies. X-ray diffraction measurements show that the deposited FTO was found to be of cassiterite type with tetragonal rutile structure, observation of peaks of different planes on an X-ray diffraction graph of CdS thin film showed that CdS film obtained were cubic structure. The main peak value of CdS thin film is seen at $2\theta = 26.505°$, which is the characteristic peak of the CdS compound(111) and the CdTe film structure was obtained at the major peak $2\theta = 24.2°$ indicating

**Corresponding author: E-mail: msaid@nwu.edu.ng;*

the preferred orientation of CdTe films along (111) direction. This confirms the formation of CdTe thin film, with (111) as the strongest preferred plane of orientation. The surface morphology of the thin films was analysed by scanning electron microscopy (SEM). The optical energy band gap of thin films are determine $\mathrm{FTO} = 3.4\mathrm{eV}, \mathrm{CdS} = 2.38\mathrm{eV}$ and $\mathrm{CdTe} = 1.62\mathrm{eV}$. The results showed that the prepared FTO, CdS and CdTe films can be used in solar energy applications.

Keywords: Spray pyrolysis; FTO; XRD; UV-vis; band gap and CdS & CdTe.

1. INTRODUCTION

Fluorine doped tin oxide (FTO), Cadmium sulfide (CdS) and Cadmium telluride $(CdTe)$ are important semiconductor materials in optoelectronic devices such as optical sensors, light-emitting diodes, transistors and photovoltaic cells [1]. In solar cells, FTO is used as transparent conducting oxide,to allows incoming light to reach the photoactive layer.

CdS is used as a window layer because it has high optical transmittance in the visible region, high optical band gap $(E_g \sim 2.4\ eV)$ at room temperature, homogeneity, compactness, crystallinity, photoconductivity as well as natural n-type electrical conductivity [2]. CdS is a II-VI semiconductor material that has two crystalline forms: the hexagonal wurtzite structure, which has greater stability, and the metastable cubic zinc blende structure [3] although $CdTe$ is a II=VI semiconductor is used as an absorber layer because of its optimal band gap of $1.45\ eV$ and it can absorbs more than 90% of obtainable photons in $1\ \mu m$ thickness, therefore $1-3\mu m$ film are adequate for thin film solar cells[4].

Concerning the fabrication of FTO, CdS and $CdTe$ thin films, different physical and chemical deposition techniques are adopted, such as electro deposition [5], chemical bath deposition [6], close spaced sublimation [7], radio frequency (RF) sputtering [8], metal organic chemical vapor deposition [9], pulsed-laser deposition [10] and spray deposition[11]. Spray pyrolysis is commonly employed for depositing FTO, CdS and $CdTe$ thin films due to its simplicity in fabrication process, low-cost and suitability for deposition of large area thin films [12]. Besides, this technique can be carried out at low temperature [13].The properties of $CdTe$ and several potential TCSs are summarized in Table 1.

This study used X-ray diffraction (XRD), scanning electron microscopy (SEM), and ultraviolet visible light to analysed the fabricated thin films for solar cell application. Morphological features, and optical features (UV-vis) were also analysed and properties such as defect, band gap and intensity were computed.

1.1 Theoretical Background

SP is a process in which a nanostructure is sprayed or injected Nano porous nebulizer onto the hot substrate in the furnace leading to decomposition of precursor to form the final desired material on the substrate. Spray pyrolysis is the aerosol process that atomizes a solution and heat the droplets to produce solid particles [15].

Advantage of spray pyrolysis technique as compared with other deposition techniques; simple and low cost thin film deposition technique, applicable to large area, deposition leads to relatively uniform and high quality coating, no high temperature are required during processing, film deposited by spray pyrolysis are reproducible giving it potential for mass production[13].

Thin films formation by spray pyrolysis technique:

- In the first step an aqueous precursor solution is converted into aerosol by spray nozzle.
- Solvent evaporation takes place.
- Vaporization of the solvent leads to precipitate formation as the droplets approaches the substrate.
- Pyrolysis of the precipitate occurs in succession before the precipitate reaches the substrate.
- When the precipitate reaches the substrate, nucleation and growth of metal oxide thin films on the substrate surface takes placed.
- Growth of the nuclei leads to formation of continuous thin layer of metal oxide.

Steps for spray pyrolysis deposition:

Atomization of the precursor solution→ Aerosol transport of the droplets → Decomposition of precursor.

Table 1. Properties of selected II-VI compound and transparent conducting semiconductor [14]

Semiconductor	Energy gap (eV)	Lattice constants (Å)	Thermal expansion coefficient$(\times 10^{-6}{}^{\circ}C^{-1})$	Electron affinity (eV)
$CdTe(cubic)$	$1.44(d)$	6.477	5.5	4.28
$CdS(hexagonal)$	$2.42(d)$	$a, 4.131$ $c, 6.116$	$5.5(\perp c-axis)$ $2.5(\parallel$ c−axis)	4.5
ZnO	$3.3(d)$	$a, 3.25$ $c, 3.21$	4.8 2.9	4.35
$ZnSe(cubic)$	$2.67(d)$	5.669	7	
$ZnS(hexagonal$	$3.66(d)$	$a, 3.819$ $c, 6.256$	$4.9-6.5$ $(\parallel$ c − axis) $4.5(\perp c-axis)$	3.9
$SnO_2:F$	$3.9-4.6(d)$	6.1		4.8

The size of the generated droplets is not related to any fluid property of the precursor solution and depends solely on the fluid charge density level qe as in

$$r^2 = \left(\frac{-\alpha}{\beta}\right)\frac{3\varepsilon_o}{q\rho_e} \quad *$$

Where ε_o the permittivity, q is charge and $\frac{-\alpha}{\beta}$ is a constant value equal to$1.0 \times 10^{-17}J$.

The mass of droplet, assuming spherical shape depends on its density.

$$m = \frac{4\pi}{3}\rho q r^3 \quad **$$

Where, r is the droplet radius and q is the droplet density. The initial leaving velocity of the droplet is an important parameter as it determines the rate at which the droplets reach the substrate surface, the heating rate of the droplet, and the amount of time the droplet remains in transport Due to its ease of production, pressure atomizers was used. A pressure atomizer uses high speed air in order to generate an aerosol from a precursor solution. Increasing the air pressure causes a direct decrease in the generated mean droplet diameter.

1.2 Structural Properties

A diffraction pattern is created when X-rays contact with a crystalline substance (phase). Every material produces a pattern; the same substance creates the same pattern every time; and in a mixture of substances, each material makes its own pattern independently of the others. By using the Bragg's diffraction condition:

$$2dsin\theta = n\lambda \quad (1)$$

(where, d = interplanar spacing, $\theta = Bragg$ angle, n = order of the diffraction, λ =1.5406 Å (wavelength of X-rays)), the lattice parameter values are calculated for different planes of all the XRD patterns and the crystallite size, constant of lattice and unit cell volume were calculated using equations (2), (3) and (4) respectively.

$$D = \frac{0.9\lambda}{\beta COS\theta} \quad (2)$$

$$a = d_{hkl}\sqrt{h^2+k^2+l^2}. \quad (3)$$

$$V_{cell} = a^3 \quad (4)$$

$$\rho_{XRD} = \frac{nM}{N_A a^3} \quad (5)$$

$$\frac{1}{d_{hkl}{}^2} = \frac{4}{3}\left(\frac{h^2+hk+k^2}{a^2}\right) + \frac{l^2}{c^2} \quad (6)$$

$$V_{cell} = 0.866a^2c \quad (7)$$

Where λ is the wavelength of X-rays, with a value of 1.5406Å, β is the full width at half the maximum and θ is the diffraction angle of the Bragg, h, k, l are the Miller indices and d_{hkl} is the inter-planar spacing, M is the molecular weight, NA is the number of Avogadro, n is the number of atoms in a unit cell.

1.3 Optical Properties

A UV-VIS spectrophotometer was used to measure the optical absorption spectra of the films placed on glass. The absorption coefficients under different wavelength photon irradiation are required, and absorption coefficients are calculated indirectly either from the absorbance or diffuse reflectance spectra (Basith, 2017).

1.4 Using Absorbance

The absorption coefficient (α) is related with absorbance and the film thickness using Beer Lambert formula.

$$\alpha = 2.303\left(\frac{A}{d}\right) \quad (8)$$

Where A is the absorbance and d is the thickness of the deposited thin film [16].

The energy of the photon in electron volt (eV) is obtained using:

$$E = \frac{hc}{\lambda} = hv \quad (9)$$

Where h is the plank constant c is the speed of light and λ is the wavelength of the incident photon and hv is the energy of the incoming photon [9].

The absorption spectra of the thin film deposited are obtained using the equation 10

$$\alpha = \frac{A\left(hv - E_g\right)^{n/2}}{hv} \quad (10)$$

Where A is a constant, E_g is the band gap energy, hv is the energy of the photon and n is a constant equal to 1for direct band gap and 4 for indirect band gap materials,

Thus, the band gap of cadmium sulphide was obtained for direct band gap as stated in equation 11

$$\alpha = \frac{A\left(hv - E_g\right)^{1/2}}{hv} \quad (11)$$

The band gap was obtained by plotting $(\alpha hv)^2$ against hv and extrapolating the graph to the point where $\alpha = 0$.

1.5 Using Diffuse Reflectance

The Kubelka–Munk function was used to compute the optical band gaps of the samples. The absorption coefficient $(\propto)$ can be related to the reflectance (r) by the following relationship for an infinite length of sample:

$$F(r) = \frac{\propto}{s} = \left(\frac{(1-r)^2}{2r}\right) \quad (12)$$

Where F(r) is the Kubelka–Munk function. 'r' is the reflectance and 's' is the scattering coefficient. $(F(r)hv)^2\ vs\ hv$ Plots were extrapolated to meet the energy axis (x-axis) corresponding to $(F(r)hv)^2 = 0$. The intercept gives the value of optical band gap of the sample [17].

2. MATERIALS AND METHODS

This section lists all the materials used and the detail procedure of the method used in the thin films growth of Fluorine doped tin oxide $(SnO_2{:}F)$, Cadmium sulphide (CdS) and $CdTe$.

All reagents used are of analytical purity and were used as ordered by Bristol scientific company Lagos, Nigeria.

2.1 Substrate Cleaning

Materials used for cleaning the substrates are 5% sodium lauryl sulphate, wool, piranha solution, spinning machine and distil water. The soda lime glass was rise in 5% sodium lauryl sulphate, wool was used to brush the soda lime glass. Then the soda lime glass was dip in piranha solution for 30minutes and rise in distil water and dry for 20 seconds by spinning at 300 0rpm.

2.2 FTO Deposition

In this study, the properties of the solution prepared for coating the FTO thin film layer which acts as a transparent conducting oxide on soda lime glass substrates are given in Table 2.

And take place according to the following equationsType equation here.

$$SnCl_4 + 4CH_3 - OH_{aq} \rightarrow SnOH_4 + 4CH_3\,Cl_g \uparrow \quad 13$$

$$Sn(OH)_4 + H_2O \rightarrow SnO_2 + 3H_2O$$

$$SnO_2 + 2HF \xrightarrow{\Delta} 2SnO_2 : F + H_2 \uparrow \quad 14$$

2.2.1 Preparation of FTO thin films

The prepared FTO solution was transferred to the spray chamber of the SP device as in equation 14. Prepared substrates were positioned in the nozzle spray area in the SP device.

The parameters used in the FTO thin film coating process are given in Table 3.

Table 2. Properties of compounds used in FTO thin film solution

Compound used	purpose
$SnCl_4$	Sno_2
HF	HF
$4CH_3 - OH_{aq}$	$volatile$
H_2O	$water$

Table 3. Parameters and values for FTO thin film coating by SP method

process parameters	process values
$nozzle\ frequency$	$120KHz$
$nozzle\ \ distance$	$1.0cm$
$solution\ flow\ rate$	$1ml/min$
$substrate\ tempreture$	$500℃$
$deposition\ time$	$10 - 20\ mins$
$carrier\ gas$	$Nitrogen\ gas$

After the positioning of the substrates, the temperature of the substrate was gradually increased to $500℃$ and spraying was started with the specified parameters. In order to compare FTO thin films with different layer thicknesses, the first samples were removed from the coating section after 10 minutes of the coating. The samples left in the coating section were sprayed again and removed after a total of 20 minutes of the coating process. After spraying, the substrates were allowed to cool at room temperature.

2.3 Etching of Glass/FTO with Electrochemical Method

Digital meter was used to check the conducting side of the glass substrate; the mask was placed on the required area of the conducting side, by connecting the negative terminal of the power supply to the FTO region and the positive terminal to the carbon rod. The area to be etched was wet with distilled water, and then aqueous zinc acetate was added on the wet area. The power supply was on at $(7.2\ to\ 15.5V)$ the positive terminal of the carbon rod was rubbed on the area wetted with zinc acetate solution until white colour appeared, drops of HCl were added on the etching region , the surface was clean with wool, HCl drops were continuously added and cleaned with wool until the area was etched. The mask was removed and the sample was allowed to dry in air. (Why you sue etching) (etching was done for feature used in the research)

2.4 Cadmium Sulfide Thin Film Deposition

Spray pyrolysis is a chemical technique that involves spraying an aqueous solution onto a high-temperature substrate. To make CdS thin films, an aqueous solution of Cadmium acetate dihydrate Cd(CH 3 COOH) 2.2H 2 O and Thiourea (NH 2)_2 CS were employed as Cd and S sources, respectively, and were derived from a mixture of;

Weight of $Cd(CH_3COOH)_2.2H_2O = \frac{266.53\times0.1\times50ml}{1000} = 1.33265g$ (15)

Weight of $CH_4N_2S = \frac{76.12\times0.1\times50}{1000} = 0.3806g$ (16)

The precursor solution and carrier gas (air) assembly connected to the spray nozzle, the reaction chamber in which the substrate was heated, the pumping and exhausting gas scrubbing systems, and a temperature controller with a Copper-Constantan thermocouple to control the substrate temperature make up the deposition setup. The solution was sprayed onto a glass substrate that had already been cleaned. The temperature of the substrate was kept constant at 400°C. The normalized distance between the spray nozzle and the substrate was adjusted to 20 cm. The pressure of the carrier gas (air) was kept constant at 1 bar. The solution flow rate was kept constant at 0.5 ml/m throughout the experiment.

To compare CdS thin films of different layer thick nesses, the first samples were extracted from the coating segment after 30 minutes of coating and the samples left in the coating section were sprayed again and removed after a total of 60 minutes of the coating process. The grown CdS films colour changes with the time from greenish yellow to bright yellow as shown on

Plate 1. The possible chemical reaction that takes place on the heated substrate to produce CdS.

$$Cd(CH_3COOH)_2.2H_2O + (NH_2)_2CS + H_2O \rightarrow CdS \downarrow + CO_2 \uparrow + CH_4 \uparrow + steam \quad (17)$$

2.5 Cadmium Telluride Deposition

Deposition procedure was covered in five stages.

Stage I; $0.056g\ TeO_2$ Was added to $100ml\ NH_3$ at room temperature, the solution was stir using magnetic stirrer until solution turn colourless.

Stage II; $10.66g\ Cd(CH_3COOH)_2.2H_2O + 18.6g\ EDTA$ disodium salt solution was prepared in $50ml$ deionised water and stirring was continued until milky colour appeared, $5ml$ Hydrazine was added to the mixture and stirring continued and deionised water was added to keep the PH content, Deionised water was continued added until the solution reached $200ml$ and stirring was continued till the solution was fully dissolved and became crystal clear.

Step III; the resulting solution was put into two necks round bottom flask on the lab tech mantle heater set at $200℃$. The solution was heated for a time of six hours and was allowed to cool at room temperature. The resulting solution was separated by centrifuging at $4000rpm$ for $3minutes$, and the centrifuging was repeated five times.

Step IV; the solution was divided into two equal parts in test tubes by weighing on analytical digital balance. The two test tubes were then placed on a centrifuge model 800 machine to centrifuge for three $3minutes$ at $4000rpm$. this process was repeated five times. The centrifuging is for proper separation. The pair of $CdTe$ solutions were mixed together and rinsed with saturated Cadmium Chloride $CdCl_2$ in N-methyl-2 Pyridine NMP.

Stage V; before the deposition of $CdTe$ solution on the SLG substrate, the spray chamber was purged with nitrogen gas for 15 min. In addition, nitrogen gas was used as a carrier gas for spraying the final precursor solution on substrates. The films were deposited on thoroughly cleaned substrates at 300°C using the following processing parameters: I spray gun nozzle to substrate distance=20cm, (ii) spray solution concentration=0.1M, (iii) carrier N 2 gas flow rate=10l/min, (iv) deposition time=20 minutes, and (v) solution flow rate=5 m/min. After completing the $CdTe$ thin film coating process which lasted 20 minutes by spray pyrolysis method, The films were cooled naturally to the room temperature. The chemical reaction that takes place in the chamber;

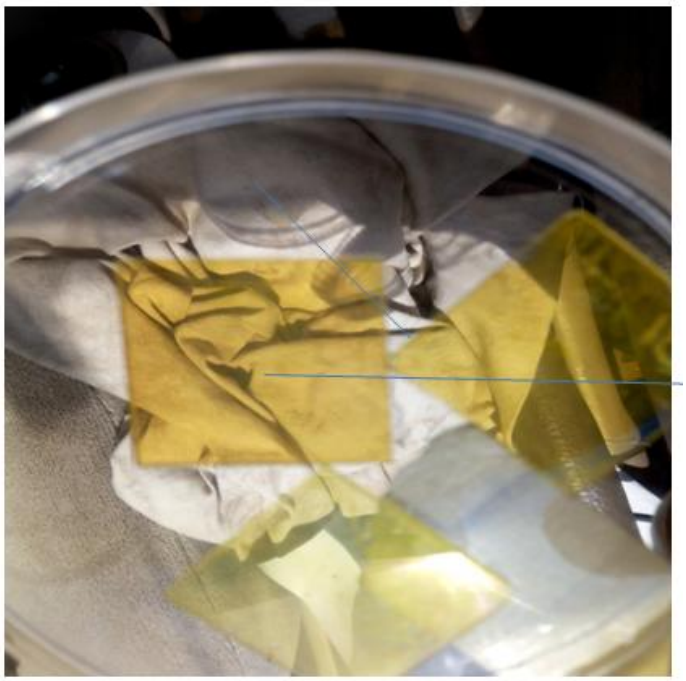

Plate 1. Visual study of CdS samples at deposited at $30minutes\ and\ 60minutes$

$$Cd^{2+} + Te + 2e^{-} \rightarrow CdTe \quad (18)$$

2.6 Details of Characterization

The structural characterization of the films was carried out using X-ray diffractometer EMPYREAN (Kaduna, NGRL) system. The instrument uses a Cu anode material for X-ray generation (V = 45 kV, I = 40 mA) with Cu K-Alpha 1 (λ = 1.54060 (Å)) and Cu K-Alpha 2 radiation (λ = 1.54443 (Å)) emitted with an intensity ratio of 0.50000. The angular range of the patterns collected between $4 \leq 2\theta° \leq 80$ with a step size of $0.0260°$ and scan step time $13.7700s/°$. The instrument helped in determining the type of crystal lattice and intensities of diffraction peaks,. The optical analysis were carried out using $750\ UV -$ visible spectrophotometer in range $300 - 1100nm$ where the absorbance of each of the samples was obtain and other optical properties were obtained by calculation and the values of thickness of resultant films were obtained by using the profilometer. This two measurement were carried out at Sheda Science and Technology Complex, Abuja. morphological study of CdS and FTO thin films were carried out using Scanning electron microscope (SEM), Camera model; Phenom (katsina, UMYU)

3. RESULTS AND DISCUSSION

In the XRD characterization of $FTO, CdS\ and\ CdTe$ thin films deposited with spray pyrolysis method, X-ray diffraction patterns were obtained by X-ray diffractometer EMPYREAN (Kaduna, NGRL) using Cu-Kα line $(\lambda = 154060\ A°)$. The XRD graph of FTO thin films with a deposition temperature of $500℃$ is shown in Fig. 1.

From the XRD graph given in Fig. 1, there are peak values with different intensities and different widths. The results show that the films were observed to be of cassiterite type with the tetragonal rutile structure. the lattice parameter values are calculated for different planes of the XRD patterns and the diffract gram were found to be in good agreement with the previous work of [18]also found to be very close to the standard data given in JCPDS data file No.41–1049 for FTO phase.

Table 4 present the calculated values of the crystallite size, constant of lattice and unit cell volume using equations (4), (5) and (6) respectively.

Fig. 2. displays the Xray diffraction patterns (XR D) of CdS thin films prepared using the deposition technique of spray pyrolysis at consta nt substrate temperature $400℃$ at different deposition time. The XRD patterns in Fig. 2 were compared with Joint Committee on Powder Diffraction Standards (JCPDS) file no. $01 - 075 - 1546$. The XRD pattern reveals the presence of CdS. The peaks at $26.505\ (111)$ correspond to the cubic phase, of CdS. The sharp diffraction peaks indicate the formation of well crystallized film. And the calculated crystallized size in Table 5 are in good agreement with the reported values obtained by[19].

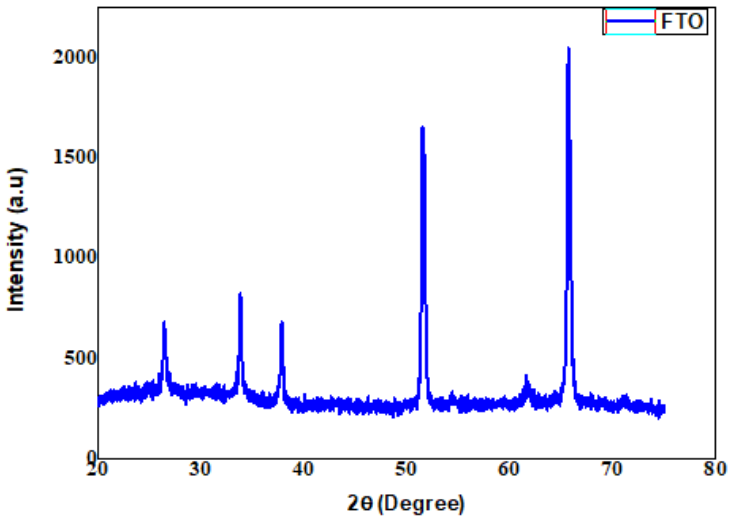

Fig. 1. X-ray diffraction patterns (XRD) of FTO

Table 4. Lattice constant (a), Crystallite size(D), Volume of unit cell(V_{cell}), X-ray mass density (ρ_{XRD}) for FTO

Sample name	$2\theta°$	$d_{hkl(Å)}$	$\beta°$	a(Å)	c(Å)	c/a	$D(nm)$	V_{cell}(Å)^3
FTO	35.55	2.5229	0.212	4.76	3.47	0.73	14.81	68.09

Table 5. Peak list for xrd of FTO

$position\ 2\theta°$	$Height\ (cts)$	$FWHM\ 2\theta°$	$d-spacing$ (Å)	$intensity$(%)
26.39	319.14	0.1536	3.37742	18.59
33.79	506.03	0.1791	2.65232	29.59
37.81	403.11	0.2047	2.37922	23.45
51.46	1355.85	0.1872	1.77437	78.97
51.63	1235.01	0.1245	1.77315	71.93
61.55	84.41	06240	1.50528	4.92
65.63	1716.87	0.1872	1.42142	100.00

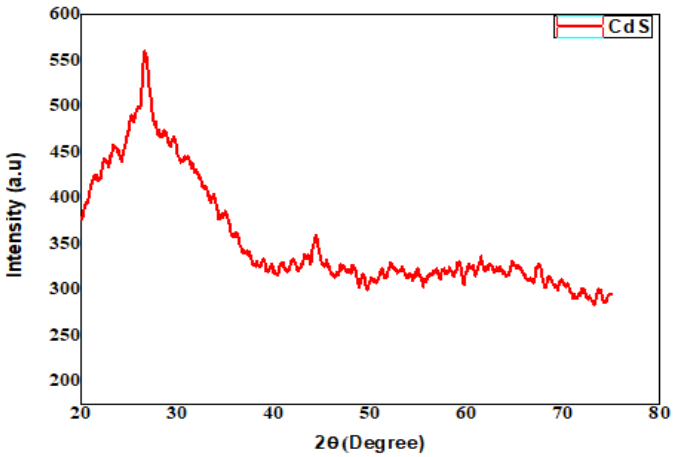

Fig. 2. X-ray diffraction patterns (XRD) of CdS

The XRD spectra of $CdTe$ thin films was displayed in Fig. 3 and it consists of a few sharp peaks at 2θ positions the high intensity reflection in $CdTe$ film structure was obtained at the major peak $2\theta = 24.2°$ indicating the preferred orientation of $CdTe$ films along (111) direction. This confirms the formation of $CdTe$ thin film, with (111) as the strongest preferred plane of orientation. The obtained XRD spectra of $CdTe$ was matched with standard JCPDS card 15–0770 thus confirmed the composition of the film to be $CdTe$ and giving stable zinc-blende crystalline structure.

3.1 Morphological Studies of FTO and CdS

The morphological studies were performed to ensures homogeneity of the crystal grown. SEM images of FTO and CdS thin films deposited on glass substrate are shown in Figs 4a and 4b. The morphological analysis of CdS and FTO thin films was carried out using a scanning electron microscope (SEM). The deposited samples was found to have a spherical and somewhat homogenous surface shape and extremely adherent to the glass substrates which is in agreement with the reported value by [21]. The average particle size of $FTO\ at\ 2000magnification$ thin films was$134\mu m$. The bigger grain with less grain boundaries was obtained by choosing the approximate annealing temperature, ambient condition and annealing time of 1hour.

3.2 Thickness Measurement with Profilometer

The thickness values of FTO and CdS films deposited at different substrates deposition time are found to be for FTO $200nm$ while for

$360nm$. The thickness of film was found to be increasing with increasing the deposition time. The same deposition parameters are employed to create films at varied substrate deposition times. All of the films are naturally cooled to ambient temperature after each deposition. As a result, the increase in film thickness observed as the substrate deposition time increases could be related to densification of the films.

Table 6. Lattice constant (a), Crystallite size(D), volume of unit cell(V_{cell}), X-ray mass density (ρ_{XRD}) for CdS

SAMPLE NAME	$2\theta°$	$d_{hkl(Å)}$	$\beta°$	$a(Å)$	$D(nm)$	$V_{cell}(Å)^3$	$\rho_{XRD}(g/cm^3)$
CdS	26.51	3.3602	0.499	5.82	16.35	197.14	4.868

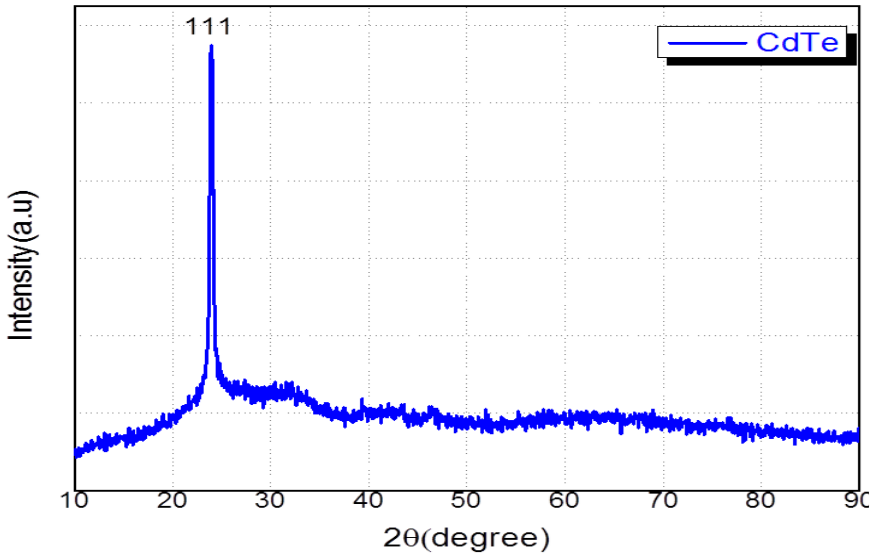

Fig. 3. display the X-ray diffraction pattern of $CdTe$ thin film

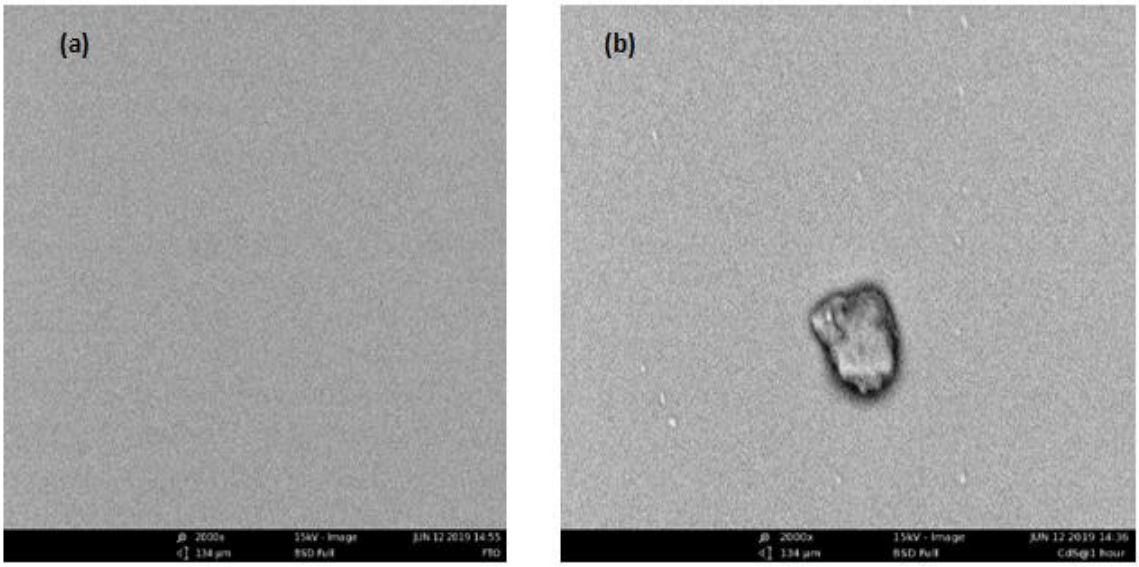

Fig. 4. SEM micrograph of (a) FTO $at\ 2000magnification$ thin film (b) $CdS\ thin\ film\ 2000magnification$ for 1h

3.3 Optical Properties Studies

Optical absorption studies were carried out on the FTO, CdS films and absorption spectrum was shown in the Fig.5 and 6 these studies were carried out to find out the optical band gap of the semiconductors.

Using an optical absorbance method, the band g ap of FTO and CdS thin films produced by sprayp yrolysis method was determined, and band gap g raphics were prepared. The FTO thin film optical band gap value was calculated from the graph in Fig 5 by extrapolating the linear portion of the graph to the energy axis and was found to be$3.4eV$, which is in agreement with the reported value by [20] and which is very near to standard value of the band gap forFTO and The CdS thin film optical band gap value was also calculated from the graph in Fig 6 by extrapolating the linear portion of the graph to the energy axis and found to be $2.38eV$, which is in agreement with the reported value by [21] and which is very near to standard value of the band gap forCdS.

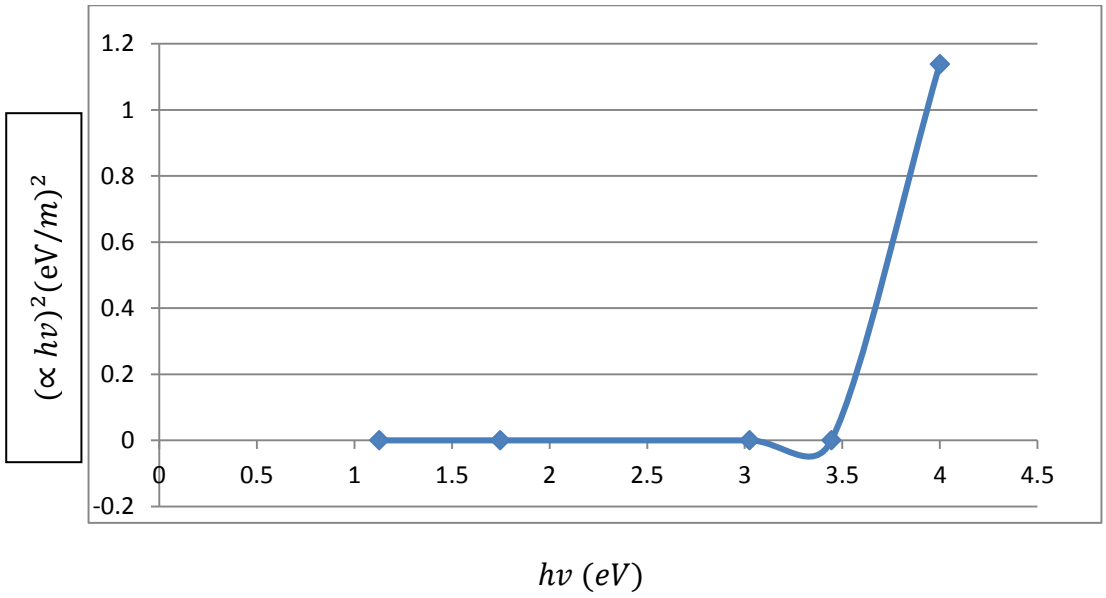

Fig. 5. a graph of $(\alpha hv)^2$ Vs hv to determine the optical band gap of FTO

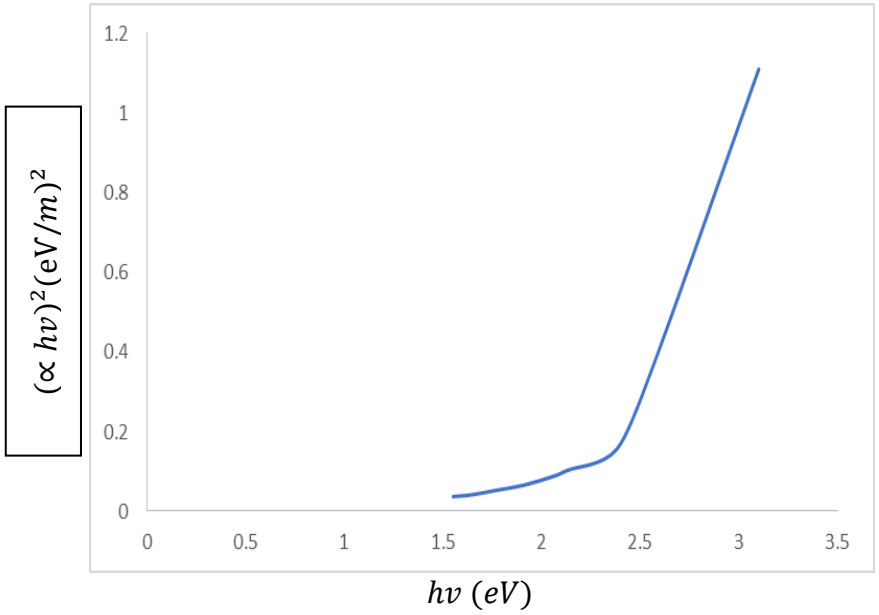

Fig. 6. a graph of $(\alpha hv)^2$ Vs hv to determine the optical band gap of CdS thin film

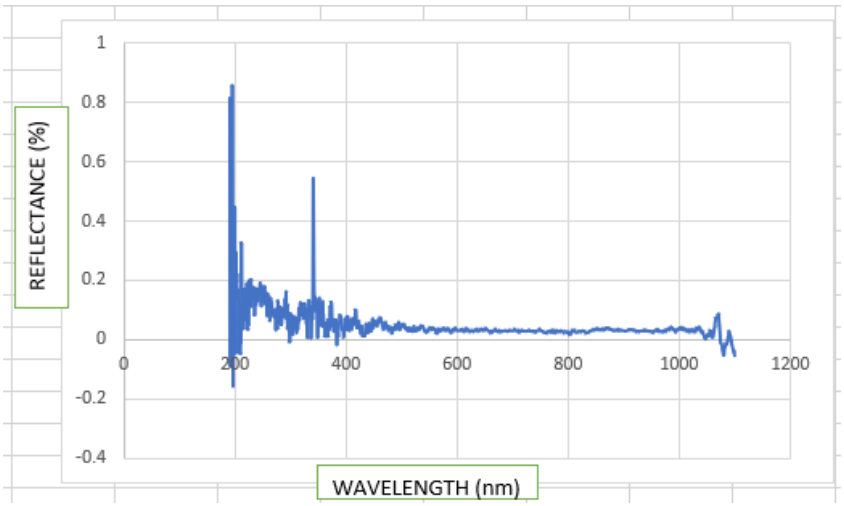

Fig. 7. Diffused reflectance spectra of cadmium telluride thin film

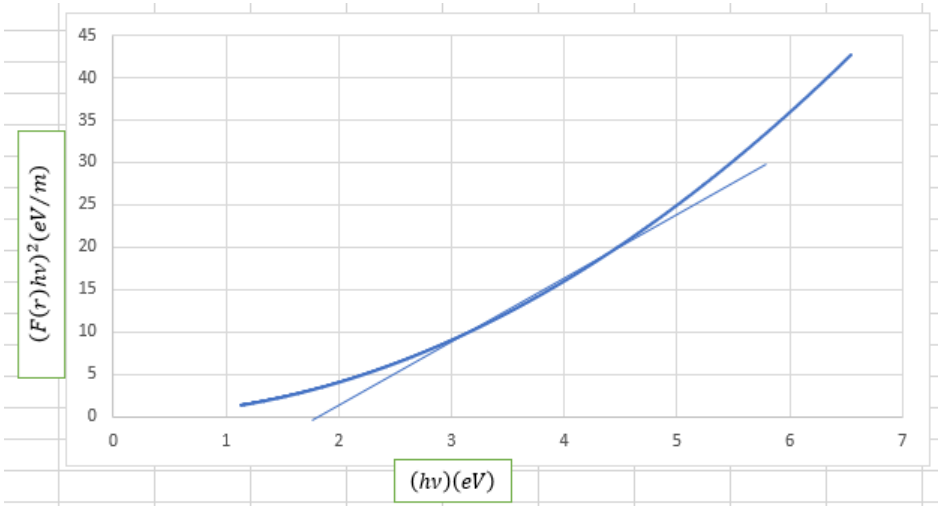

Fig. 8. optical band gap of cadmium telluride thin film

Optical Properties measurements for $CdTe$ thin film were done at room temperature using a UV-750 Series spectrophotometer with average scan 10 in the wavelength range of $300-1100\ nm.$

From diffused reflectance spectra Fig. 7, It was found that the magnitude of reflectance of $CdTe$ films vary periodically with wavelengths. Multiple oscillations occur on the reflectance curves due to interferences among multiple reflected waves. As the wavelength increases, oscillation period of these films changes. Thus, the reflectance characteristics of $CdTe$ films are strongly dependent on the wavelength of electromagnetic spectra. The optical band gaps of the sample were calculated using Kubelka–Munk function is shown in Fig. 8.

$(F(r)hv)^2\ vs\ hv$ Plots were extrapolated to meet the energy axis (x-axis) corresponding to $(F(r)hv)^2 = 0$ and was found to be$1.62\ eV$ which was in agreement with reported value by [10] The intercept gives the value of optical band gap of the sample (Fig. 8).

4. CONCLUSION

Spray pyrolysis has been proven to be a cost-effective and simple-to-use process for producing non-scratchable, well-adhesive, and uniformly thick nano-crystalline FTO, CdS, and CdTe films. The structural and optical properties of the deposited film layers were investigated, and both films were found to be polycrystalline and to have direct band gap characteristics of 3.4, 2.38, and 1.62 eV for FTO, CdS, and CdTe, respectively.

FTO thin films formed at a constant substrate temperature of 500°C were found to be of the cassiterite type with a tetragonal rutile structure, whilst CdS thin films were found to be of the rutile type. The peaks at 26.505 (111) correspond to the cubic phase of CdS deposited at 400°C, as revealed by its XRD pattern.

The band gap values for FTO and CdS films obtained were found to be consistent with previously reported band gap values for cassiterite type with tetragonal rutile FTO and cubic CdS phase. As a result of the spray pyrolysis approach utilized in this study, FTO and CdS films can be used as a parent conductive oxide and a window layer in hetero-junction solar cells.

The band gap of $CdTe$ thin films as measured $1.62\ eV$ using optical reflectance (UV–visible spectrophotometer) method. Thus, the usability of $CdTe$ thin films produced by spray pyrolysis method as absorbing the material in photovoltaic cells has been shown.

Rely I got doubt why the Author study all this material to gathers.

This paper is part of the series of papers performed on this research.

DISCLAIMER

The products used for this research are commonly and predominantly use products in our area of research and country. There is absolutely no conflict of interest between the authors and producers of the products because we do not intend to use these products as an avenue for any litigation but for the advancement of knowledge. Also, the research was not funded by the producing company rather it was funded by personal efforts of the authors.

COMPETING INTERESTS

Authors have declared that no competing interests exist.

REFERENCES

1. Faraj MG, Eisa MH, Pakhuruddin MZ. Physical Properties of Spray Pyrolysed Cadmium Sulfide Thin Films Deposited on Different Polymer Substrates. 2019;14: 10633–10641. Available:https://doi.org/10.20964/2019.11.11
2. Sharma RK, Jain K, Rastogi AC. Growth of CdS and CdTe thin films for the fabrication of n-CdS/p-CdTe solar cell. Current Applied Physics, 2003;3(2–3):199–204. Available:https://doi.org/10.1016/S1567-1739(02)00201-8
3. Gunjal SD, Khollam YB, Arote SA, Jadkar SR, Shelke PN, Mohite KC. Structural , Optical and Electrical Properties of Spray Pyrolysis Deposited CdS Films. 2015;9–15. Available:https://doi.org/10.1002/masy.201400046
4. Bonnet D, Meyers P. Cadmium-telluride — Material for thin film solar cells;1998.
5. Dharmadasa IM, Bingham PA, Echendu OK, Salim HI, Druffel T, Dharmadasa R, Abbas A. Fabrication of CdS/CdTe-Based Thin Film Solar Cells Using an Electrochemical Technique. 2014;380–415. Available:https://doi.org/10.3390/coatings4030380
6. Hiie J, Dedova T, Valdna V, Muska K. Comparative study of nano-structured CdS thin films prepared by CBD and spray pyrolysis: Annealing effect. Thin Solid Films, 2006;511–512:443–447. Available:https://doi.org/10.1016/j.tsf.2005.11.070
7. Rahman KS, Harif MN, Rosly HN, Kamaruzzaman MI Bin, Akhtaruzzaman M, Alghoul M, Amin N. Influence of deposition time in CdTe thin film properties grown by Close-Spaced Sublimation (CSS) for photovoltaic application. Results in Physics. 2019;14:102371. Available:https://doi.org/10.1016/j.rinp.2019.102371
8. Shao M, Fischer A, Grecu D, Jayamaha U, Bykov E, Contreraspuente G, Bykov E. Radiofrequencymagnetronsputtered CdS / CdTe solar cells on sodalime glass Radio-frequency-magnetron-sputtered CdS / CdTe solar cells on soda-lime glass. 2014;3045(1996):1994–1997. Available:https://doi.org/10.1063/1.116834
9. Kartopu G, Turkay D, Ozcan C, Hadibrata W, Aurang P, Yerci S, Irvine SJC. Solar Energy Materials and Solar Cells Photovoltaic performance of CdS / CdTe junctions on ZnO nanorod arrays. 2018;176:100–108. Available:https://doi.org/10.1016/j.solmat.2017.11.036

10. Kulkarni R, Rondiya S, Pawbake A, Waykar R, Jadhavar A. Structural and optical properties of CdTe thin films deposited using RF magnetron sputtering. Energy Procedia, 2017;110:188–195. Available:https://doi.org/10.1016/j.egypro.2017.03.126
11. Gunjal SD, Khollam YB, Arote SA, Jadkar SR. Structural , Optical and Electrical Properties of Spray Pyrolysis Deposited CdS Structural , Optical and Electrical Properties of Spray Pyrolysis Deposited CdS Films;2015. Available:https://doi.org/10.1002/masy.201400046
12. Jamil S, Ahmad-bitar RN. Original article A study of the optical bandgap energy and Urbach tail of spray-deposited CdS : In thin films. Integrative Medicine Research. 2013;2(3):221–227. Available:https://doi.org/10.1016/j.jmrt.2013.02.012
13. Rmili A, Ouachtari F, Bouaoud A, Louardi A, Chtouki T, Elidrissi B, Erguig H. Structural , optical and electrical properties of Ni-doped CdS thin films prepared by spray pyrolysis. Journal of Alloys and Compounds. 2013;557:53–59. Available:https://doi.org/10.1016/j.jallcom.2012.12.136
14. Garba D. Research and development of CdTe based thin film PV solar cells;2011.
15. Singh VK. Thin Film Deposition by Spray Pyroysis Techniques. Emerging Technologies and Innovative Research (JETIR). 2017;4(11):1–9.
16. Cao H, Wang G, Zhang S, Zhang X, Rabinovich D, Carolina N. Growth and Optical Properties of Wurtzite-Type CdS Nanocrystals. 2006;45(13):5103–5108.
17. Singh S, Kalia G, Singh K. Effect of intermediate oxide (Y 2 O 3) on thermal, structural and optical properties of lithium borosilicate glasses. Journal of Molecular Structure. 2015;1086:239–245. Available:https://doi.org/10.1016/j.molstruc.2015.01.031
18. Optik S, Nipis F, Oksida T, Florin T. Structural, Optical and Electrical Properties of Fluorine Doped Tin Oxide Thin Films Deposited Using Inkjet Printing Technique. 2011;40(3):251–257.
19. Lee J. Influence of substrates on the structural and optical properties of chemically deposited CdS films. 2007;515:6089–6093. Available:https://doi.org/10.1016/j.tsf.2006.12.097
20. Banyamin ZY, Kelly PJ, West G, Boardman J. Electrical and Optical Properties of Fluorine Doped Tin Oxide Thin Films Prepared by Magnetron Sputtering. 2014;732–746. Available:https://doi.org/10.3390/coatings4040732
21. Ikhmayies SJ, Ahmad-bitar RN. A Comparison between the Electrical and Optical Properties of. 2010;4(1):111–116.

Peer-review history:
The peer review history for this paper can be accessed here:
https://www.sdiarticle4.com/review-history/71413